drones

Article

Performance of Individual Tree Segmentation Algorithms in Forest Ecosystems Using UAV LiDAR Data

Javier Marcello [1,*], María Spínola [1], Laia Albors [2], Ferran Marqués [2], Dionisio Rodríguez-Esparragón [1] and Francisco Eugenio [1]

[1] Instituto de Oceanografía y Cambio Global, IOCAG, Unidad Asociada ULPGC-CSIC, 35017 Las Palmas de Gran Canaria, Spain; maria.spinola101@alu.ulpgc.es (M.S.); dionisio.rodriguez@ulpgc.es (D.R.-E.); francisco.eugenio@ulpgc.es (F.E.)
[2] Signal Theory and Communications Department, Universitat Politècnica de Catalunya, BarcelonaTech, 08034 Barcelona, Spain; laia.albors@upc.edu (L.A.); ferran.marques@upc.edu (F.M.)
* Correspondence: javier.marcello@ulpgc.es

Abstract: Forests are crucial for biodiversity, climate regulation, and hydrological cycles, requiring sustainable management due to threats like deforestation and climate change. Traditional forest monitoring methods are labor-intensive and limited, whereas UAV LiDAR offers detailed three-dimensional data on forest structure and extensive coverage. This study primarily assesses individual tree segmentation algorithms in two forest ecosystems with different levels of complexity using high-density LiDAR data captured by the Zenmuse L1 sensor on a DJI Matrice 300RTK platform. The processing methodology for LiDAR data includes preliminary preprocessing steps to create Digital Elevation Models, Digital Surface Models, and Canopy Height Models. A comprehensive evaluation of the most effective techniques for classifying ground points in the LiDAR point cloud and deriving accurate models was performed, concluding that the Triangular Irregular Network method is a suitable choice. Subsequently, the segmentation step is applied to enable the analysis of forests at the individual tree level. Segmentation is crucial for monitoring forest health, estimating biomass, and understanding species composition and diversity. However, the selection of the most appropriate segmentation technique remains a hot research topic with a lack of consensus on the optimal approach and metrics to be employed. Therefore, after the review of the state of the art, a comparative assessment of four common segmentation algorithms (Dalponte2016, Silva2016, Watershed, and Li2012) was conducted. Results demonstrated that the Li2012 algorithm, applied to the normalized 3D point cloud, achieved the best performance with an F1-score of 91% and an IoU of 83%.

Keywords: LiDAR; ULS; DEM; CHM; tree segmentation; forest; watershed; Dalponte; Silva; Li

Citation: Marcello, J.; Spínola, M.; Albors, L.; Marqués, F.; Rodríguez-Esparragón, D.; Eugenio, F. Performance of Individual Tree Segmentation Algorithms in Forest Ecosystems Using UAV LiDAR Data. *Drones* **2024**, *8*, 772. https://doi.org/10.3390/drones8120772

Academic Editor: Eben N. Broadbent

Received: 29 October 2024
Revised: 4 December 2024
Accepted: 16 December 2024
Published: 19 December 2024

1. Introduction

Forested areas play a fundamental role in maintaining biodiversity and regulating biogeochemical cycles, essential for the planet's ecological health. These regions function as carbon sinks, mitigating climate change by absorbing atmospheric carbon dioxide. Additionally, forested areas provide crucial habitats for a vast number of species, many of which are endemic and unable to thrive in other environments. The biodiversity within forests is vital for ecosystem balance, as species interactions contribute to overall stability and resilience. Furthermore, forests significantly influence the hydrological cycle, affecting precipitation patterns and water quality, which is critical for freshwater supply. Deforestation and forest degradation pose serious threats and, therefore, the sustainable management of forested areas is imperative for ensuring long-term ecological stability and human well-being [1].

Traditional methods to monitor forests, such as field surveys and inventories, have long been utilized to gather data on tree species, density, and health. These methods, while providing detailed and localized information, are often labor-intensive, time-consuming,

and limited in spatial extent. In contrast, modern technologies, such as sensors in remote sensing platforms, have revolutionized forest monitoring [2,3]. These instruments enable the detection of changes in forest cover, biomass, and biodiversity with high precision and over large areas, facilitating real-time monitoring and rapid response to deforestation and forest degradation. Combining traditional and modern methods can enhance the accuracy and efficiency of forest monitoring, providing a robust framework for assessing forest health, planning conservation strategies, and ensuring sustainable forest management.

Over the past few decades, remote sensing has predominantly utilized passive sensors on board aircraft and satellites. However, the recent advent of Unmanned Aerial Vehicles (UAVs) has introduced the capability for significantly higher spatial resolution observations. The primary trade-offs among these platforms revolve around cost, as well as spatial and temporal resolutions. Satellites offer open access data, but with spatial resolutions around 250 m if daily imagery is required. Resolutions up to 10 m are possible but with a revisit of 5 days (e.g., Sentinel-2 constellation). On the other hand, commercial satellites offer meter-level resolution, though this comes at the cost of reduced temporal frequency and additional expenses. However, the ongoing revolution in the domain of small/micro/cube satellites is altering the landscape of data availability, offering higher temporal and spatial resolutions at an affordable cost (e.g., PlanetScope). Aircraft, on the other hand, can deliver high-resolution active or passive observations, but at a substantial cost. Finally, UAV technology is advancing rapidly, presenting an optimal trade-off between cost and very high resolution for local area monitoring.

In forest areas, the use of passive and active remote sensing sensors has become integral, providing complementary approaches to gather comprehensive data. LiDAR (LIght Detection And Ranging) offers several advantages over SAR (Synthetic Aperture Radar) and passive multispectral (MS) or hyperspectral (HS) data for forest monitoring, providing high-resolution, three-dimensional data on forest structure, capturing precise information on canopy height, density, and understory composition. This level of detail is critical for accurate biomass estimation, carbon stock assessment, and detailed forest inventories. In contrast, SAR, while useful in all-weather conditions and capable of penetrating through some vegetation depending on the operated frequency band, typically offers lower spatial resolution, and its analysis is complex. MS or HS data, on the other hand, depend on sunlight and clear weather, which can limit its availability and consistency. Moreover, optical sensors primarily capture surface reflectance, lacking the ability to penetrate dense canopies and provide detailed vertical structure information for forest monitoring. Anyway, with the integration of LiDAR structural data, SAR roughness and texture, and the spectral information from multispectral and hyperspectral sensors, it is now possible to gain a deeper understanding of vegetation health, species composition, and forest dynamics. This data fusion allows for more accurate ecosystem assessments, supporting improved decision-making for sustainable land management and conservation efforts.

As indicated, LiDAR systems are powerful tools for forest analysis. In particular, various types of LiDAR systems are nowadays employed based on specific application needs [4]: Unmanned Aerial Systems LiDAR (ULS), Airborne LiDAR Systems (ALS), Mobile LiDAR Systems (MLS), and Terrestrial LiDAR Systems (TLS). ULS systems are mounted on UAVs, offering high spatial resolution, density, and flexibility for capturing detailed forest data. ULS is particularly useful for small to medium-sized areas and provides excellent data for analyzing canopy structure, tree height, and biomass. Its ability to fly at low altitudes allows for capturing fine-scale details. In fact, ULS offers distinct advantages over MLS and TLS, providing unparalleled flexibility and accessibility, capable of surveying remote and difficult-to-reach areas by flying over rough terrains and dense vegetation that ground-based systems cannot easily access [4]. In contrast, MLS is restricted to linear routes accessible by vehicles, limiting its coverage and efficiency, while TLS, though delivering ultra-high-resolution data, is labor-intensive and time-consuming, making it less suitable for large-scale surveys. Additionally, ULS is often more cost-effective for extensive forest monitoring compared to the logistical demands of MLS and the intensive fieldwork

required for TLS. Note that LiDAR systems are also available on satellite platforms, such as the Global Ecosystem Dynamics Investigation (GEDI) mounted on the International Space Station [5] or the Advanced Topographic Laser Altimeter System (ATLAS) on board the ICESat-2 satellite [6]. Unfortunately, the resolution they can offer is not adequate to address accurate local vegetation studies.

A processing methodology is essential to transform raw LiDAR data into valuable information products that support forest conservation. The workflow for processing LiDAR typically involves several steps with the aim of deriving the Canopy Height Model (CHM) by subtracting the Digital Elevation Model (DEM) from the Digital Surface Model (DSM). The CHM precisely delineates the height of vegetation above ground level, and this vertical vegetation structure data are essential to monitor forest health and dynamics over time, etc.

Specifically, tree segmentation plays a crucial role in modern forest management. Accurate tree segmentation allows for the identification of individual trees within a forest, which is essential for monitoring tree growth, health, and species composition. This information is vital for sustainable forest management practices and supports carbon stock assessments by providing detailed data on tree volume and biomass, which are key for estimating carbon sequestration potential. Furthermore, tree segmentation can be used to monitor forest regeneration, detect early signs of disease or pest infestations, and assess the effectiveness of conservation efforts. When dealing with ULS data, segmentation is an essential processing step for accurate individual tree analysis, as it enables precise identification and measurement of tree attributes in complex forest structures. Segmentation algorithms are employed to characterize individual trees within the CHM or the normalized LiDAR point cloud.

Several approaches exist for tree segmentation in LiDAR data, ranging from simple height-based thresholding methods to more complex machine learning algorithms. Traditional techniques have mainly used methods such as valley delineation, watershed segmentation, and template matching [7,8]. These traditional methods often require manual parameter adjustment and are sensitive to variations in image quality. Machine and deep learning models have emerged as powerful alternatives for individual tree segmentation [9–11]. A recent review of the latest trends on tree classification and segmentation using UAV data analyzed a total of 144 papers published in the period 2013–2023 [12]. Authors conclude that most works use RGB or multispectral cameras for tree segmentation and classification. Focusing on LiDAR scanners, segmentation mostly uses unsupervised machine learning techniques, and the following methods are mostly considered: local maxima, watershed, Voroni tessellation, region growing, and point cloud segmentation. On the other hand, another recent review on individual tree crown detection and delineation, but specifically with convolutional neural networks (CNN) [13], indicates that the most used data type is high-resolution RGB images taken from UAVs. In particular, for object detection (e.g., individual trees), region-based CNNs (R-CNN), Mask R-CNNs [14,15] and YOLO [16,17] approaches are becoming popular, as well as PointNet++ [18]. Despite the development of numerous image segmentation techniques in recent years, there remains a lack of consensus on the optimal methods for different data and forest types [8,13].

In this context, after a comprehensive review of the state of the art of individual tree segmentation focused on LiDAR data, Table 1 summarizes some representative studies in natural areas, mainly published in impact journals in the last 3 years. In accordance with the focus of the article, the review was limited to aerial systems (ALS and ULS), disregarding terrestrial LiDARs. The table provides information about the forest type considered, the LiDAR data used, the preprocessing techniques applied, and the relevant information about the segmentation algorithms implemented. There is a wide variety of studies covering different types of forests (temperate, alpine, etc.), with coniferous and eucalyptus forests predominating. Regarding the type of LiDAR platform and sensor, as expected, to address analysis at the tree level, recent works mostly consider high-density LiDAR data from UAVs instead of the use of airplanes or helicopters. The cloud density varies between a few and thousands of points per square meter. Regarding the preprocessing steps to label the

ground points and to generate the DEM, CHM, or the normalized point cloud, the most used software tools are LIDAR360 and LidR, but other applications such as CloudCompare or LAStools are also considered. Finally, the predominant algorithms for tree detection and segmentation using the CHM were, mainly, the Local Maxima Filtering and Watershed, followed by Silva2016 and Dalponte2016. Several different algorithms were selected for the segmentation using the point cloud; Li2012 was the most used, followed by Layer Stacking, MeanShift, etc. Note that few works still apply deep learning approaches. In this context, a review paper about tree crown detection and delineation with Convolutional Neural Networks [13] indicates that CNN models showed significant improvements in accuracy, but performance varied across different forest environments and data types. In particular, ResNet was the most used default backbone. It is important to highlight that the work concludes that most CNN models were mostly applied to high-resolution RGB imagery, in line with the results provided in Table 1, due to the lack of open LiDAR segmented databases to train and test the models.

Table 1. Review of the state of the art of individual tree segmentation using LiDAR data.

Author (Year)	Forest Type	Platform and Sensor	Preprocessing (Software)	Segmentation Algorithms
Yan et al. (2024) [19]	Eucalyptus	UAV: 288 pts/m^2	- Ground classification: progressive morphological filter (LIDAR360 and LidR)	- CHM: Watershed, Local Maximum - Point cloud: Euclidean Distance Clustering, Layer Stacking
Zhan et al. (2024) [20]	Temperate forestand other types: coniferous, eucalyptus, alluvial	UAV: - 50 pts/m^2 - 90 pts/m^2 - 100 pts/m^2	- Ground classification: cloth simulation filtering (CloudCompare)	- CHM: Dalponte2016, Silva2016, Parkan 2018. - Point cloud: Treetool, Mean Shift, Li2012 and the proposed hierarchical filtering and clustering - Deep Learning: Xiang2023
Saeed et al. (2024) [21]	Pines	Airplane: 3 pts/m^2	- DEM: TIN (TerraScan) - CHM (LidR)	- CHM: Dalponte2016, Silva2016, Watershed - Point cloud: Li2012, Adaptive mean-shift, Density Based
Yu et al. (2024) [22]	Coniferous forest, mixed forest and broadleaf forest	UAV (Zenmuse-L1): 197 pts/m^2	- Ground classification: progressive TIN - DEM: inverse distance weighted interpolation (LIDAR360)	- CHM: adaptive crown shaped algorithm, local maximum, region growing - Point cloud: Li2012
Wang et al. (2024) [23]	Camellia oleifera	UAV (DJI Matrice300 RTK, LiAir VH2)	- DEM: TIN	- CHM: Watershed - Point cloud: Li2012, Layer Stacking
Wielgosz et al. (2024) [24]	Different types: coniferous, eucalyptus, alluvial	UAV: 10, 100, 500, 1000 pts/m^2	Data already preprocessed	- Deep Learning: Xiang2023
Liu et al. (2024) [25]	Different forest types in Alpine regions	UAV: 10, 20 and 30 pts/m^2 Airborne: 20.97 pts/m^2	Data already preprocessed	- CHM: Local maxima, Watershed - Point cloud: spectral clustering algorithm (vertical profiles)
Nemmaoui et al. (2024) [26]	Mediterranean forest (pines)	PNOA Airborne (LEICA ALS80-HP): 3.5 pts/m^2	- Cloud normalization and CHM generation (LidR)	- CHM: Dalponte2016, Silva2016, Watershed - Point cloud: Li2012
Lin et al. (2024) [15]	Taiga and Tundra (coniferous)	Airborne (Leica ALS70-HP): 0.8–1.1 pts/m^2	- DEM (TIN) and CHM (ENVI)	- CHM: Mask R-CNN and Multi-Scale Adaptive Segmentation - Point cloud: Li2012
Jarahizadeh and Salehi (2024) [17]	Forest with different tree types and densities.	UAV (DJI Martrice 300 RTK and Zenmuse-L1)	- Ground classification (KNN) and CHM generation	- CHM: Yolo v7 and v3
Xiang et al. (2023) [27]	Different types: coniferous, eucalyptus, alluvial	UAV (Riegl VUX-1 UAV and Mini-VUX): 500–3500 pts/m^2	Data already preprocessed	- Deep Learning: input data generator + deep neural network CNN (U-Net) + post-processor
Chen et al. (2023) [28]	Very dense mixed forest	Helicopter: 160 pts/m^2	- Ground classification: progressive TIN - DEM: Inverse Distance Weighted interpolation (LIDAR360)	- CHM: Multiresolution segmentation - Point Cloud: Li2012
You et al. (2023) [29]	Mixed broad-leaved tree plantation	UAV (DJI Matrice 300RTK and Zenmuse L1): 440 pts/m^2	- Ground classification and DEM: (LIDAR360) DSM and CHM: (LidR)	- CHM: Watershed
Tao et al. (2023) [30]	Artificially planted *Picea crassifolia*	UAV (DJI Martrice 300 RTK and Zenmuse-L1): 1300 pts/m^2	- Ground classification (Cloth simulation filter), DEM (Kriging) and CHM generation (LIDAR360)	- CHM: Watershed - Point cloud: Li2012
Liu et al. (2023) [31]	Broadleaf mixed plantation	UAV (BB4 U, AU20): 105 pts/m^2	- DEM (Kriging) and cloud normalization	- Point cloud: PointNet++, Li2012, Layer Stacking
Ma et al. (2022) [32]	Eucalyptus and fir trees	UAV (DJI Matrice 600 and RIEGL VUX-1LR): >300 pts/m^2	- Gound classification: progressive TIN (LIDAR360)	- CHM: Watershed. Local Maximum - Point cloud: Li2012, Layer Stacking
Farajelahi et al. (2022) [33]	Dense conifers forest	Airplane: 0.7 pts/m^2	- Ground classification: Cloth Simulation Filter (Cloud Compare)	- CHM: reconstruction and morphologic operations
Dalla-Corte et al. (2022) [34]	Eucalypt stands	UAV (GatorEye): 1500–2500 pts/m^2	- Ground classification: Adaptive TIN (LASTools)	- CHM: Local Maximum Filter and Dalponte2016

Considering these challenges, this study undertakes a comparative analysis of algorithms for individual tree detection and crown delineation using ULS data. We considered two possible sources of input data (the CHM raster image and the normalized 3D point cloud) used by the algorithms to identify the most effective approaches. In this context, the main contributions of this work can be summarized as follows:

- Conduct an evaluation of the most effective preprocessing techniques to classify ground points and to generate the corresponding Digital Elevation Model (DEM) using ULS data.
- Undertake an exhaustive and up-to-date review of recent studies that focus on the segmentation of individual trees in forest areas using LiDAR data.
- Develop and provide an openly accessible ULS-annotated dataset to facilitate the evaluation and benchmarking of individual tree segmentation algorithms in a coniferous forest plot.
- Carry out a comparative analysis of prominent segmentation algorithms in scenarios characterized by different levels of forest complexity.

2. Materials and Methods

2.1. Study Area

According to the last report on the state of the Spanish protected natural spaces (Europarc 2023) [35], Spain is the European country that contributes the most to the Natura 2000 Network (27.4% of the country surface) and that has the most biosphere reserves in the world (53). Specifically, it accounts for 36.7% of the protected land area and 12.3% of its marine surface. Due to its isolation and topography, the Canary archipelago, located in the Atlantic Ocean off the northwest African coast, stands out for its richness in biodiversity of endemic species. For this reason, the Canary Network of Protected Natural Areas [36] was created, which consists of 146 natural areas that together constitute, approximately, 40% of the surface of the archipelago. This network covers diverse ecosystem types, reflecting the unique characteristics of each individual island. It was created to contribute to human well-being and the maintenance of the biosphere through the conservation of nature and the protection of esthetic and cultural values present in natural spaces.

This research analyzes the Garajonay and Caldera de Taburiente national parks. Garajonay, located on La Gomera island, is renowned for its ancient laurel forests, a relic of the Tertiary period, offering a unique ecosystem and rich biodiversity [37]. In contrast, Caldera de Taburiente on La Palma features a massive volcanic crater, lush pine forests, and landscapes shaped by erosion and volcanic activity. Figure 1 shows both protected natural areas of the Canary Islands. It can be appreciated the complexity of Garajonay to identify individual trees due to the extremely high density of vegetation.

2.2. Data

In this study, we utilized LiDAR point clouds captured by the Zenmuse L1 sensor. This high-performance sensor can generate data at a rate of 240,000 points per second, thereby ensuring detailed and comprehensive coverage. It boasts a vertical and horizontal accuracy of 5 cm and 10 cm, respectively, which contributes to the precision of the data collected. The sensor was deployed on the DJI Matrice 300RTK UAV, a reliable and efficient platform for aerial data collection. The flight altitude was approximately 60 m and took place on 28 June 2023 (Garajonay) and on 1 October 2023 (Taburiente), covering an area of 340 m $\times$ 240 m in Garajonay and 250 m $\times$ 250 m in Taburiente. The system achieved a mean point density of 500 points/m^2, providing a rich dataset for our analysis.

Ground truth information was necessary to compare and validate the segmentation algorithms applied to the LiDAR data. For the Taburiente park, since there was no previous field data available for this area, a plot of 47 m $\times$ 58 m containing heterogeneous scenarios was selected to assess the precision of the algorithms, with clearly separated individual trees and others with overlapping crowns. A total of 24 trees were counted, specifically pines. In addition, areas with lush undergrowth of great height were observed, exceeding, in some

cases, 3 m in height. Their precise coordinates were obtained, and a detailed photographic and video report was made, captured from different angles and distances, to carry out a precise manual segmentation on the normalized point cloud to generate the reference dataset for the comparison of the different algorithms analyzed for the location and segmentation of trees available at https://doi.org/10.5281/zenodo.14051045 (accessed on 29 October 2024). Regarding the Garajonay national park, the conservation manager provided detailed field data from a plot within the study area. The field data covers a plot of 40 m × 40 m in the northern part of the image with a total of 154 trees with their associated information (precise location using a submeter RTK GNSS receiver, trunk diameter using a caliper, total height using a Vertex hypsometer, etc.). Figure 2 shows photographs, the true color images of both areas and the ground truth information included in the orange and yellow boxes. Taburiente, displayed in the upper row, shows the park's most representative species is the Canary Island pine (*Pinus canariensis*), which is the vegetable symbol of the island and the reference ground truth. Garajonay, due to the complexity of the relief of the summits of La Gomera, has a great variety of environments that favor the presence of different types of laurisilvae, such as laurel (*Laurus novocanariensis*), tile (*Ocotea foetens*), vinátigo (*Persea indica*), barbusano (*Apollonias* barbujana), etc., as well as areas of fayal-brezal (*Morella faya-Erica arborea*).

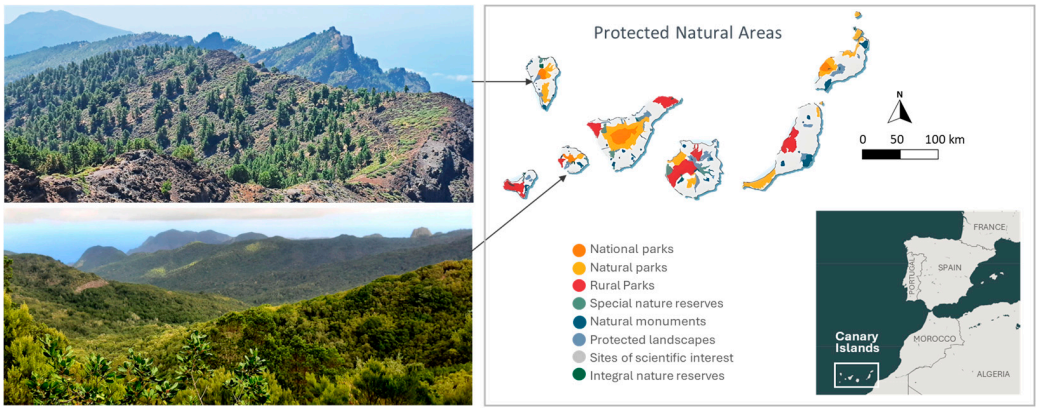

Figure 1. Map of the protected natural areas of the Canary Islands and photographs of the National Parks of Caldera de Taburiente in La Palma (**top left**) and Garajonay in La Gomera (**bottom left**).

2.3. Methodology

A complete processing protocol is essential to transform raw LiDAR clouds into valuable information products that support forest conservation. The general workflow for processing LiDAR data typically involves several steps: (i) data acquisition to collect the raw LiDAR data, (ii) filtering to remove noise and irrelevant data points; (iii) classification to label each cloud point into ground, vegetation, and other categories; (iv) model generation to create continuous models from the classified points, using interpolation, to derive the Digital Elevation Models (DEMs), Digital Surface Models (DSMs), and the Canopy Height Models (CHMs) by subtracting the DEM from the DSM. Figure 3 shows the general overview of the methodology applied to extract individual tree parameters. The blue boxes represent processes or data involving the 3D point clouds, while the green boxes are related to the raster images. As shown in the diagram, segmentation algorithms are applied to either 3D or 2D data, depending on the context.

2.3.1. Preprocessing

After the preliminary filtering and removal of noise and outliers, one of the most important steps in LiDAR point cloud preprocessing is the classification of the ground points. The distinction between soil and non-soil classes will allow the correct generation of the Digital Elevation Model. There are several algorithms developed for ground point classification, which are necessary when the data provider does not deliver the classified

point clouds. Each of these algorithms offers unique advantages in terms of accuracy and computational efficiency for ground point classification in LiDAR data. This paper studies and evaluates the application of three prominent algorithms used for this purpose:

(i) The Progressive Morphological Filter (PMF) algorithm [38] classifies ground points in LiDAR data by iteratively applying morphological operations to remove non-ground points. It progressively increases the window size to filter out higher objects, effectively distinguishing ground from non-ground points.

(ii) The Cloth Simulation Function (CSF) algorithm [39] simulates a cloth draped over an inverted LiDAR point cloud. By analyzing the interactions between the cloth and the points, it identifies ground points based on the final shape of the cloth, which conforms to the terrain.

(iii) The Triangular Irregular Network (TIN) algorithm [40] constructs a TIN from initial ground points by connecting them with triangular facets and iteratively densifies it by adding new points that meet specific criteria, effectively refining the ground surface model.

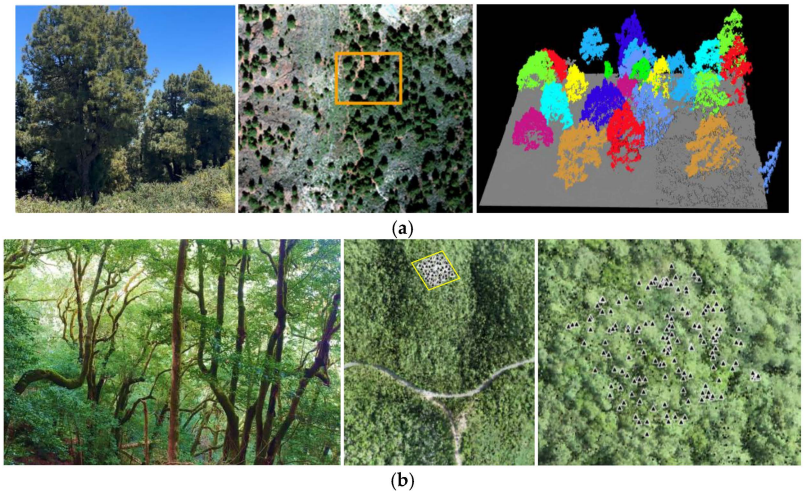

Figure 2. Vegetation, true color imagery, and ground truth data for the parks of (**a**) Caldera de Taburiente and (**b**) Garajonay.

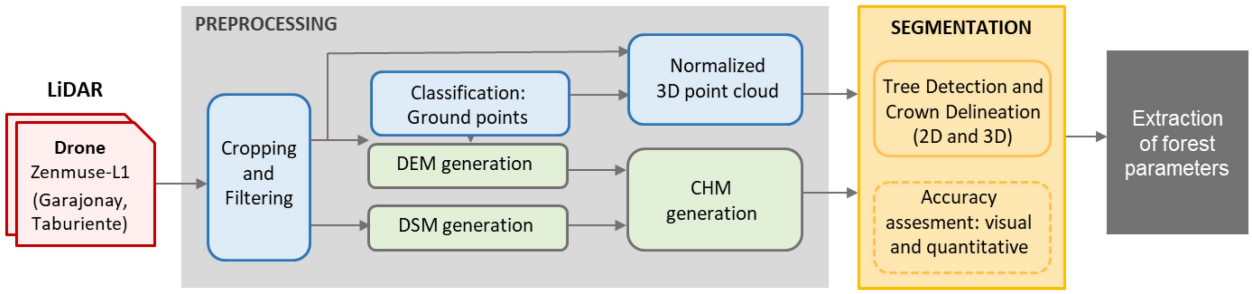

Figure 3. Simplified methodology of the individual tree detection and crown delineation using LiDAR data for the extraction of forest parameters.

The generation of the Digital Elevation Model is the subsequent step after the classification of the ground points. It is a raster image that reflects the terrain of the surface under study. There are several algorithms that have been developed to obtain the DEM, which are based on taking the cloud points previously classified as ground and applying spatial interpolation techniques to calculate ground points in the unsampled areas. There are three main algorithms that are the ones evaluated in the present work:

(i) The Triangular Irregular Network (TIN) approach is also used to generate the DEM from those classified ground points. In this case, a Delaunay triangulation is used, which employs a traditional point-by-point insertion [41].
(ii) Inverse Distance Weighting (IDW) [42] estimates unknown values based on the weighted average of known points, with closer points having more influence. This method is simple and effective but can produce less smooth surfaces in areas with sparse data.
(iii) Kriging [43] is another popular interpolation technique that not only considers the distance between points but also the spatial correlation among them. It provides more accurate and statistically robust results, especially in areas with complex terrain, but is computationally intensive.

The Digital Surface Model represents the topography of the Earth's surface, including all natural and man-made features such as trees, buildings, and other structures. Thus, DSMs capture the heights of all objects on the surface. For its generation, it uses the same algorithms as those presented in the previous paragraph for DEM generation, but taking all the information present in the point cloud.

Finally, the Canopy Height Model represents the height of vegetation, such as trees, above the ground surface. It is created by subtracting the DEM, which represents the bare ground, from the DSM, which includes the altitude of all surface features. This results in a 2D model that highlights the vertical structure of the canopy, providing valuable information for ecological and forestry studies.

As presented in Figure 3, a normalized 3D cloud will be, as well, generated. It refers to a LiDAR point cloud where the elevation values have been adjusted relative to the ground level. This normalization process helps in accurately analyzing the heights of objects above the ground, such as buildings and vegetation, by removing the influence of terrain variations.

2.3.2. Segmentation

Tree segmentation techniques generally fall into two categories: individual tree detection and individual crown delineation [13]. Individual tree detection identifies tree locations or treetops as point features, while individual crown delineation outlines individual crowns as polygon areas. Traditional methods for tree detection include local maximum filtering, image binarization, template matching, and scale analysis. For individual crown delineation, widely used methods include valley-following, region-growing, and watershed segmentation. Some crown delineation methods require individual tree detection as a preliminary step.

As mentioned, despite numerous advancements in image analysis techniques, there is no consensus on the optimal methods for different image types and forest conditions.

After reviewing recent works on tree segmentation with LiDAR data (Table 1), we decided to choose the software tools LIDAR360 (version 8.0) and LidR (version 4.1.0), as they have proven to be reliable and, mainly, because they have been used predominantly in both preprocessing and in segmentation tasks, incorporating most of the tree delineation methods (Watershed, Silva2016, Dalponte2016, and Li2012). Specifically, LIDAR360 is a robust, commercial solution that offers advanced point cloud processing capabilities, including effective algorithms for individual tree identification, canopy height modeling, and tree crown delineation. It is user-friendly and designed for large-scale forestry applications. On the other hand, LidR, an open-source package in R, is highly flexible and widely used in research settings. It provides state-of-the-art tools for tree segmentation, including customizable algorithms that allow users to fine-tune parameters for optimal tree detection in various forest types.

The segmentation methodology applied is illustrated in the block diagram in Figure 4, where the software tool used in each case is highlighted with a different color code. As shown in Figure 4, it is generally necessary to apply algorithms that locate individual trees before applying the segmentation or crown delineation techniques. As mentioned, in the

present work, we compared algorithms widely used by the remote sensing community and available in conventional software tools (LIDAR360 and LidR). This comparison was carried out in Taburiente, since we have the manually segmented cloud using field data as a reference to analyze the performance of each approach.

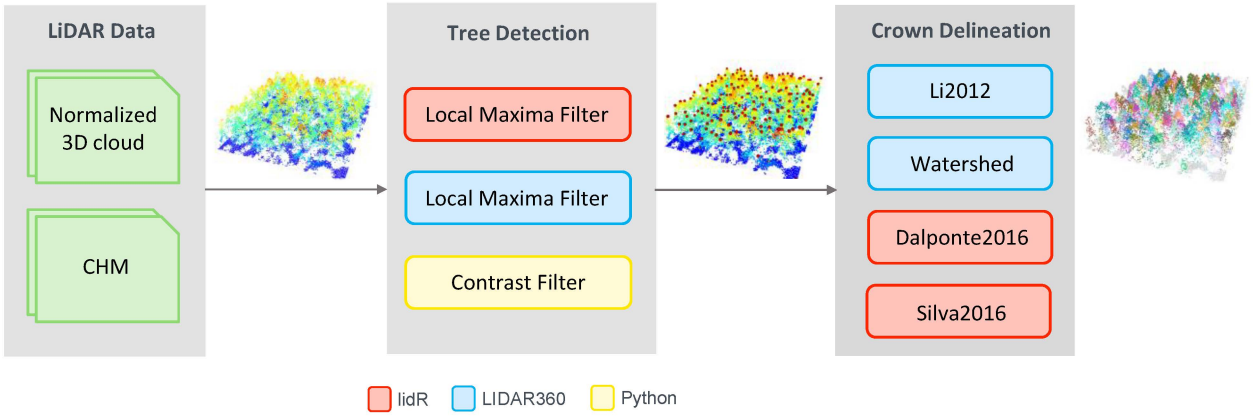

Figure 4. Selected algorithms to compare the performance of individual tree detection and crown delineation methods (Software implementation is represented by red, blue, and yellow colors and discussed in Section 3).

The most commonly used algorithm for tree location is the Local Maximum Filter (LMF) [44]. This technique is based on searching for height points with local maximum values. It is necessary to define the size of the search window, which can be circular or square. To avoid selecting maxima in areas of no interest, such as undergrowth, the filter can use a minimum height threshold. In addition, we tested the Contrast Filter (CF) [45] as it was successfully applied to deal with similar 3D data in other computer vision areas. This algorithm is based on the application of classical mathematical morphology techniques and, specifically, on the dilation reconstruction operation for the localization of maxima. It first creates a marker image by subtracting a constant value C from the original image, so that the contrast of the whole image is lowered, and local maxima are highlighted. The value of C acts as a contrast threshold that determines how different pixels must be from their adjacencies to be considered local maxima. Therefore, the lower the value of C, the greater the number of localized maxima detected.

Next, for tree segmentation and crown delineation, algorithms that have the CHM as input and those that input the normalized 3D point cloud were considered. The algorithms belonging to the first group are Dalponte2016 [46], Silva2016 [47] and Watershed [48], while Li2012 [49] was selected among those that operate with the normalized point cloud. Basically:

(i) Dalponte2016 is a seed and region-growing algorithm that works on the basis of CHM. First, local maxima are labeled as initial regions from which a tree crown can grow. Next, the heights of the four adjacent pixels are extracted. The user must define two parameters: a percentage with respect to the height of the local maximum and a maximum difference. An adjacent pixel will be added to the region only if the vertical distance is less than the percentage and less than the maximum difference. This evaluation of the neighboring pixels is repeated iteratively with all the points.

(ii) Silva2016 integrates clustering and point filtering techniques, focusing on segmenting complex forest structures efficiently on the CHM. It is an algorithm based on seeds and Voronoi diagrams. First, starting from each seed, a buffer of variable radius is applied, defined as a parameter, to delimit the initial area of the tree crown. Once the crown has been delimited, the data are divided using Voronoi diagrams, allowing the creation of polygons that represent the area of influence of each tree, thus isolating each tree crown individually. Then, each polygon is taken, and the points whose height is less than a specified percentage of the maximum height of the detected tree

are discarded to eliminate low-height noise. Finally, the tree crowns are delimited by identifying and grouping the pixels that belong to each tree, according to the polygons generated and filtered.

(iii) Watershed simulates water flow across a landscape. It consists of applying the concept of watershed ("water basin") at the lowest point of each of the CHM regions and flooding them, generating barriers in the segmentation when different watersheds meet. During the application of this algorithm, it is necessary to define the following parameters: maximum and minimum tree height, buffer size in pixels, and crown base height threshold. The buffer size is a threshold to control the block size to avoid memory overflows. The value of this parameter must be greater than the maximum crown area.

(iv) Li2012 uses a region-growing approach, starting from local maxima to iteratively segment tree crowns based on height and proximity. It works directly with the normalized 3D point cloud and assumes that there are always gaps between trees.

The optimization process to select the appropriate parameters in the detection or segmentation algorithms is a crucial step to ensure accurate and effective results. Unfortunately, there is no universal range of values for each parameter, and, depending on the study area or the type of LiDAR data, it will be necessary to conduct tests iteratively until the optimal value is achieved. In any case, as detailed in Section 3.2, certain information about the ecosystem under study (e.g., tree height, canopy structure, crown diameter, maximum understory height, etc.) can help filter out unsuitable data and narrow down the range of certain parameter values.

2.3.3. Accuracy Assessment

The accuracy assessment of tree segmentation models is an important step in the methodology and involves both qualitative and quantitative evaluations of mapped tree locations and crown delineations. For qualitative evaluation, visual inspections are typically conducted to compare the mapping results with subjective reference data, such as true color aerial imagery or the canopy height model. This method provides a direct analysis of the spatial distribution of errors and the overall performance of the segmentation algorithms. On the other hand, quantitative evaluations often use metrics common in computer vision to assess individual tree detection or crown delineation from various perspectives [9,32,50]. The traditional metrics selected in this work are:

(i) Precision (p) measures the accuracy of correctly identified trees among all detected trees by calculating the ratio of true positives (TP: number of correctly detected or segmented trees) to the sum of true positives and false positives (FP: number of incorrectly detected or segmented regions. Thus, the number of other objects misdetected as trees).

$$p = \frac{TP}{TP + FP} \tag{1}$$

(ii) Recall (r) assesses the proportion of actual trees that are correctly detected by the algorithm. It reflects the algorithm's ability to identify most of the trees present in the LiDAR data. It is the ratio of true positives to the sum of true positives and false negatives (FN: number of missed target trees that were not segmented).

$$r = \frac{TP}{TP + FN} \tag{2}$$

(iii) $F1$-Score is the harmonic mean of precision and recall, providing a single metric that balances both. It is particularly useful when the dataset has an uneven class distribution or when both false positives and false negatives are equally important.

$$F1 = 2 \times \frac{p \times r}{p + r} \tag{3}$$

(iv) Intersection over Union (*IoU*) measures the overlap between the predicted tree crown and the ground truth crown. It is calculated as the area of intersection divided by the area of union. *IoU* is commonly expressed in percentage, where 0 indicates no overlap while 100 a perfect matching. Multiple *IoU* thresholds can be used to provide a detailed view of the algorithm's performance.

$$IoU = \frac{Predicted \cap Ground\ Truth}{Predicted\ \cup Ground\ Truth} \tag{4}$$

These metrics, when used in combination, provide a comprehensive evaluation of tree segmentation algorithms and help to understand the strengths and weaknesses of different algorithms, guiding improvements, and ensuring accurate forest inventory and management.

Other less usual metrics used in different segmentation works, depending on the application, are the Root Mean Square Error (*RMSE*), which quantifies the differences between the predicted and actual tree counts or crown areas, and the Coefficient of Determination (R^2), which measures the proportion of variance in the ground truth data that is explained by the predicted data. It is a statistical measure that indicates the goodness of fit of the algorithm's predictions. Finally, the Overall Accuracy (*OA*) calculates the proportion of correctly identified tree crowns out of the total number of crowns in the dataset.

$$RMSE = \sqrt{\frac{\sum_{i=1}^{n} (\hat{y}_i - y_i)^2}{n}} \tag{5}$$

$$R^2 = \frac{\left[\sum_{i=1}^{n} (y_i - \overline{y})(\hat{y}_i - \overline{\hat{y}})\right]^2}{\sum_{i=1}^{n} (y_i - \overline{y})^2 \sum_{i=1}^{n} (\hat{y}_i - \overline{\hat{y}})^2} \tag{6}$$

$$OA = \frac{TP}{TP + FP + FN} \tag{7}$$

where n is the number of trees; y_i and $\hat{y}_i$ are the observed and predicted values for tree i; $\overline{y}$ and $\overline{\hat{y}}$ are the observed and predicted mean values.

2.3.4. Extraction of Information

LiDAR data captured from UAVs can provide a wealth of information for forest analysis, enabling the extraction of several key parameters essential for forest management and research. Individual tree detection and crown delineation allow for the precise mapping of tree locations, height, and crown extents. Additionally, the volume of individual trees can be estimated. These parameters offer insights into forest structure and biomass. Other information that can be derived is canopy cover and density, analyzing the distribution and density of LiDAR returns within the canopy layer. Understory vegetation and terrain modeling are also possible, with LiDAR providing detailed ground surface models that help in understanding topography and soil erosion risks. These parameters collectively enhance our ability to monitor, manage, and preserve forest ecosystems effectively.

3. Results

Next, the main results of the tree segmentation methodology are presented. In addition, a preliminary description of the accuracy of the classification of ground points is included due to its relevance in the generation of the CHM or the normalized point cloud.

The data of Taburiente and Garajonay national parks used in this work are presented in Figure 5.

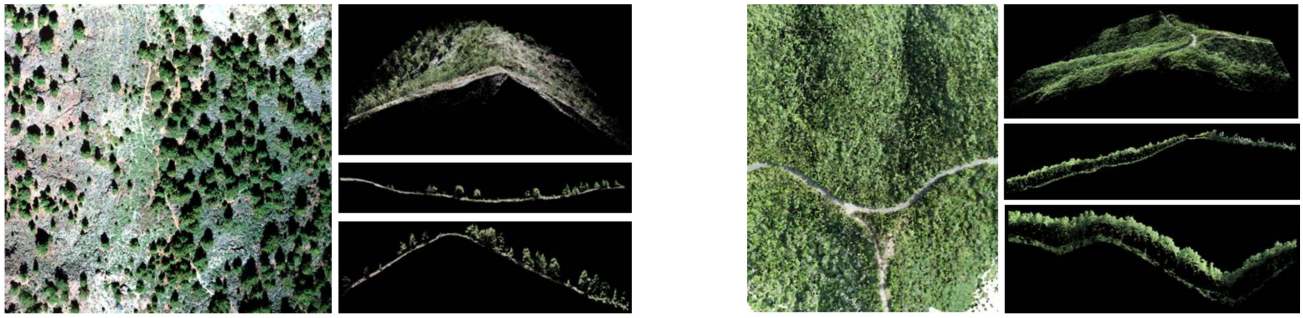

(**a**) (**b**)

Figure 5. Color composite and LiDAR data (3D cloud and examples of horizontal and vertical profiles) of: (**a**) Caldera de Taburiente and (**b**) Garajonay.

3.1. Classification of Ground Points

Accurate classification of ground points in the LiDAR cloud is crucial for deriving a precise Canopy Height Model. Ground points serve as the reference for calculating the height of the canopy by providing a detailed representation of the terrain surface. Misclassification of ground points can lead to errors in the DEM, which in turn affects the accuracy of the CHM. A precise CHM is essential for tree segmentation and, accordingly, for forestry applications. Therefore, meticulous classification of ground points is fundamental.

We chose the Garajonay park to address this issue because it presents the most challenging scenario. The extreme density of trees allows only a very limited number of LiDAR returns from the ground. Therefore, techniques with good performance in Garajonay are applicable in less complex scenarios.

For the classification of ground points, the 3 algorithms indicated in the preprocessing methodology of Section 2 were analyzed. The PMF was implemented in the R programming environment with the LiDAR data processing package lidR. The appropriate selection of the window size and the elevation difference threshold was performed to obtain good results when analyzing vertical profiles of the original cloud. The CSF algorithm was implemented with the LIDAR360 software. This tool offers predetermined parameters that adjust to three types of terrain: steep slope, gentle slope, and flat terrain. A gentle slope was chosen for our scenario, and the grid size was adjusted to 10 cm. Finally, the TIN algorithm was also applied with the LIDAR360 software using the same parameters as for CSF.

Once the ground points within the point cloud were labeled, the DEM was generated by applying the 3 presented interpolation algorithms (TIN, IDW, Kriging) to the LiDAR point cloud with the ground points classified using MPF, CSF, or TIN. The results obtained are shown in Figure 6a. Missing data can be appreciated in some areas where a minimal amount of ground points was available. In order to evaluate which strategies generate a more accurate elevation model, the DEM provided by the Spanish National Aerial Orthophotography Plan (PNOA-LIDAR) [51] was taken as a reference. The comparison between DEMs was performed in QGIS and at the same resolution of 10 cm. Figure 6b shows the error maps generated, which reveal a higher number of errors at the edges of the plot (red colors), coinciding with the areas where there is a lower density of ground points (errors above 1 m). It is observed that in the central area of the plot, all methods generate acceptable and similar results (errors below 1 m). The road that divides the plot horizontally, in all cases, is generated correctly (errors below 10 cm). This fact is reasonable since there are no trees that hinder the penetration of the LiDAR beam. At this point, it was decided that the optimal approach to implement, both in the Garajonay and in La Caldera de Taburiente, would be the TIN ground classification approach with the TIN interpolation method. This combination of techniques is the one that generates the least errors in the places of the plot with less density of points. In addition, it is important to emphasize that TIN is less demanding at the computational level, generating optimal results at reasonable speeds, unlike, for example, the Kriging interpolation method.

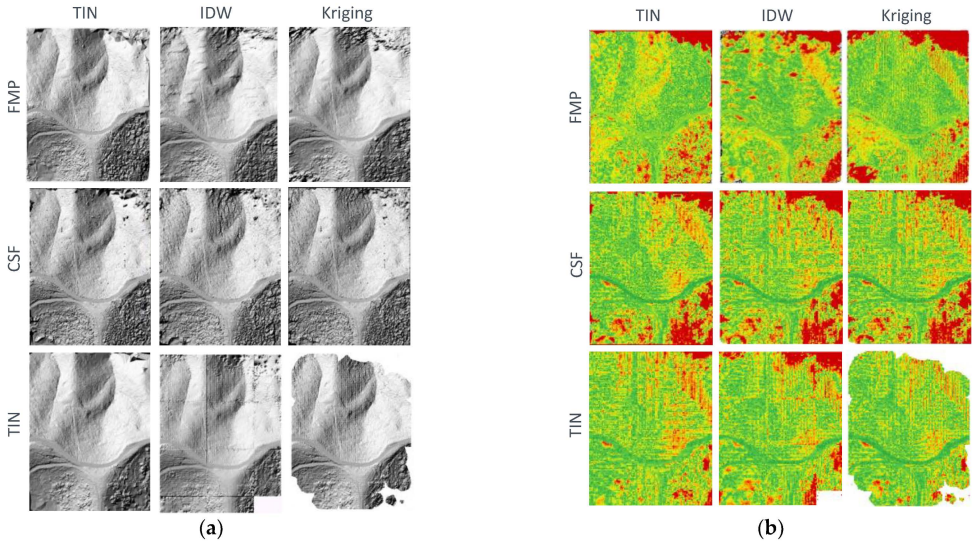

Figure 6. DEMs generated by the different combinations of ground classification and interpolation algorithms: (**a**) DEMs and (**b**) Error Maps (green colors refer to lower errors, while red colors refer to higher errors).

From the DEMs obtained using the TIN-TIN approaches, we can generate the DSM and CHM of each study site, as well as the normalized 3D point cloud. Figure 7 displays the different results obtained. As can be seen in the DSM, both forest areas are at high altitudes, above two thousand meters for Taburiente (left) and one thousand for Garajonay (right). Heights of the trees are variable, reaching up to approximately 24 m in both zones. It should also be noted, analyzing the CHM and the point cloud, that Taburiente is an excellent scenario that encompasses both clearly separated trees and others whose crowns are mixed, but, on the contrary, Garajonay is an extremely complex, dense site.

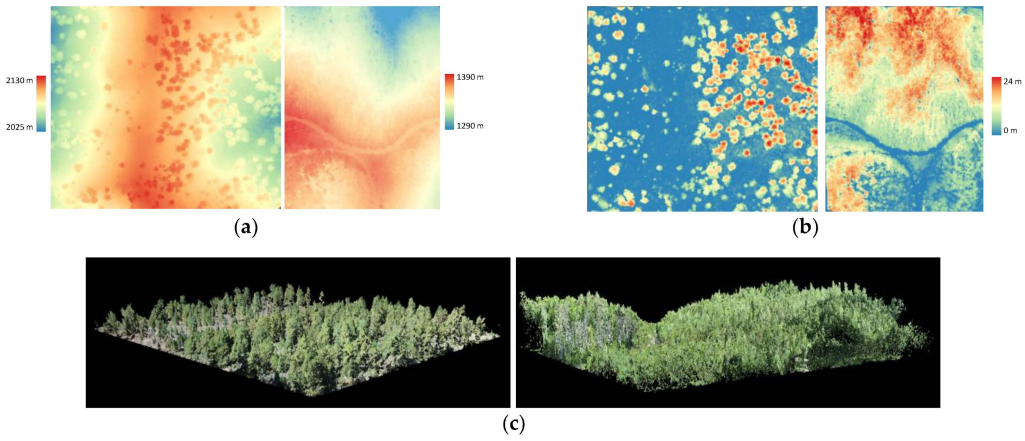

Figure 7. LiDAR models for Taburiente and Garajonay: (**a**) DEM, (**b**) CHM and (**c**) Normalized point cloud.

3.2. Individual Tree Segmentation

Once the precise height models have been obtained, it is possible to address the segmentation of individual trees. In this context, it is first necessary to apply algorithms that locate individual trees and, subsequently, those that segment the previously located trees. In this work, the most widely used algorithms were compared. This analysis was carried out in the reference plot of Taburiente, since it has the reference segmented cloud using ground truth data and lower density of trees with limited crown overlap (see Figure 2).

3.2.1. Tree Detection

The results of extracting the locations of individual trees, also called the "seed" points, by applying the algorithms listed in Figure 4, are next presented.

The Local Maximum Filter algorithm was applied in both LidR and LIDAR360 software, since LidR applies it on the normalized 3D point cloud while LIDAR360 on the CHM. The input parameters of the LMF algorithm in LidR are the diameter of the sliding window (window size, ws), in meters, where local maxima will be searched, and the minimum height for a point to be considered a local maximum. After analyzing the terrain, the minimum height of 3 m was defined, and the algorithm was run for different ws values. The parameters of the LMF algorithm in LIDAR360 are the Gaussian smoothing value (σ) and the radius (r) of the filter. For the radius, the approximate mean value of the tree crown diameter (6 m in our case) was selected, and the value of σ was varied. For the Contrast Filter method, programmed in Python, the variable parameter is the contrast value (C).

A preliminary visual analysis of the parameterization values was performed by comparing the location of the candidate trees with the actual location measured in the field campaign. After eliminating the worst candidates, the quantitative analysis was completed.

Figure 8 summarizes the main results achieved after the analysis. A wider range of values for each parameter was evaluated, but, after the visual assessment, and for the sake of clarity, only the most relevant values have been included. Graphs show the main common metrics: precision (p), recall (r) and F1-score (F1), which are calculated using the number of trees detected (DET), true positives (TP), false positives (FP), and false negatives (FN). Precision evaluates the accuracy of tree detection, whereas recall is the tree detection rate. As mentioned, the F1 score provides a full measure to compare an algorithm's overall accuracy by integrating both precision and recall. These metrics (r, p, F1) range from 0 to 100%, with 100% representing the highest accuracy. We can appreciate that CF does not provide good results irrespective of the C value, while LMF is a proper approach to detect the seeds for the segmentation techniques when the appropriate parameter values are selected.

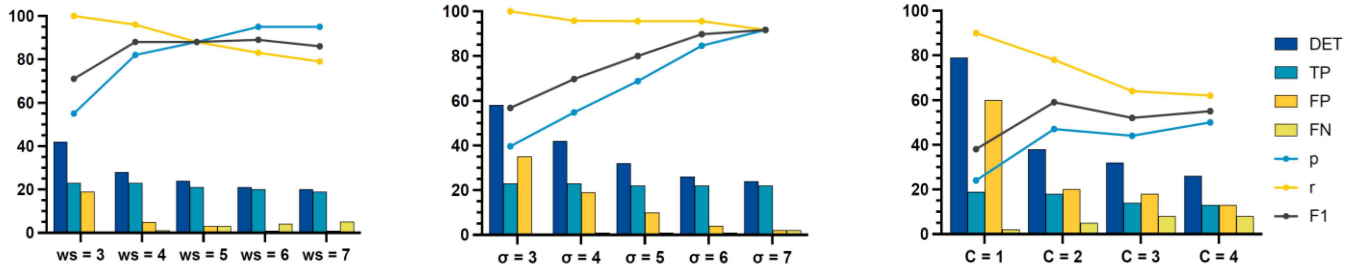

Figure 8. Performance evaluation of tree detection algorithms: (**a**) LMF-LidR, (**b**) LMF-LIDAR360 and (**c**) CF.

As detailed in Table 2, the best metric values for the LMF are given for ws = 6, with an F-score of 88.89%, and σ = 7, with an F1-score of 91.67%, in LidR and LIDAR360, respectively. Therefore, we can conclude that the LMF algorithm run in LIDAR 360 is a good choice for the detection of individual trees in LiDAR ULS datasets.

Figure 9 shows the CHM and the overlay of the seeds detected by each algorithm (black dots), using the best parameter, with respect to the real reference values, represented with the red star.

3.2.2. Tree Segmentation

Next, we present the evaluation results of the segmentation algorithms of Figure 4, using the previously identified seeds.

Dalponte2016 algorithm has different parameters to set in its execution. One is the maximum crown diameter (max_cr). To determine it, different measurements were made

in the reference plot and its value was set at 12 m. Additionally, this algorithm incorporates two other parameters to optimize its performance. On the one hand, the seed threshold (th_seed), which corresponds to the threshold according to which a pixel is added to a region if its height is greater than the height of the tree multiplied by this value. On the other hand, the crown threshold (th_cr), which determines that a pixel is added to a region if its height is greater than the average height of the current region multiplied by this value. Various values between 0 and 1 of these two parameters were tested. After analyzing the combination of both parameters using the grid search technique, it was decided that the optimal values were th_seed = 0.15 and th_cr = 0.25.

Table 2. Performance evaluation of tree detection algorithms with the best parameter values.

	LMF-LidR (ws = 6)	**LMF-LIDAR360 (σ = 7)**	**CF (C = 2)**
p	95.24%	91.67%	47.37%
r	83.33%	91.67%	78.26%
F1	88.89%	91.67%	59.02%

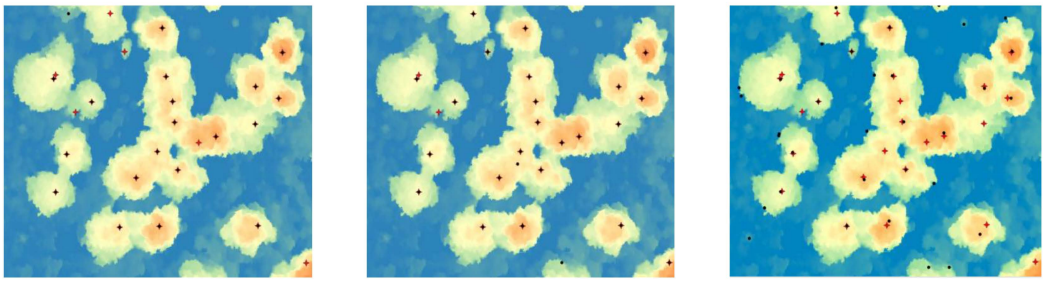

(**a**) (**b**) (**c**)

Figure 9. Reference seeds (red stars) with respect to the seeds detected by the algorithms (black dots): (**a**) LMF-LidR (ws = 6), (**b**) LMF-LIDAR360 (σ = 7) and (**c**) CF (C = 2).

Silva2016 incorporates two variable parameters, on the one hand, the maximum value of the crown factor (max_cr_factor), which is calculated as the ratio between the diameter and the height of the tree. In this case, max_cr_factor was set to 0.7 from measurements in the reference plot. The second parameter is exclusion, which is set as a threshold where pixels with height less than the exclusion value multiplied by the tree height will be removed. Different values of exclusion between 0 and 1 were tested, and the best results were obtained with the value 0.3.

The Watershed algorithm has the parameters corresponding to the Gaussian filter it applies: the smoothing (σ) and the radius (r). Again, testing values between 1 and 10, the best performance was achieved with σ = 7 and r = 6.

Finally, Li2012 works directly on the normalized point cloud and again has two variable parameters corresponding to the Gaussian filter applied, σ and r. As for Watershed, σ = 7 and r = 6 provided the best results.

Once the different segmentations were obtained, a visual and numerical analysis was carried out between the algorithms and the reference regions. In the visual evaluation, the polygon generated by each segmentation for the different algorithms and parameters (black line) was overlaid to the reference segmentation (color fill). The results using the best parameters are shown in Figure 10a.

Numerically, we first counted the number of detected, over-segmented, and undetected trees for each algorithm. Precision, recall, and F1-score were also calculated, at the pixel level in this case, to quantify the delineation capability of tree regions. In this way, the TP, FP, and FN of each tree were calculated and then, for each algorithm. The IoU was also obtained, matching each tree with its corresponding one in the reference. In case of over-segmentation, the representative tree is assumed to be the one with the largest area. Then, the intersection (common area of reference and segmentation based on LiDAR data)

and the union (areas of both polygons) are computed. Finally, the IoU is calculated as the division of the intersection by the union. A summary of some results is presented in Figure 10b. They show that segmentations on the CHM have similar performance, the best being Dalponte2016 (IoU = 74%, F1-score = 84%) and, the worst, Watershed (IoU = 62%, F1-score = 77%). However, the best overall segmentation algorithm is the one applied to the point cloud, Li2012 (IoU = 83%, F1-score = 91%), showing significantly better results comparatively. As the reference plot was carefully selected to be representative of the broader area in terms of vegetation density and distribution, as well as topography, the conclusions are generalizable to the entire region. In fact, the visual analysis of the derived segmentation regions for the entire area corroborated the quantitative results.

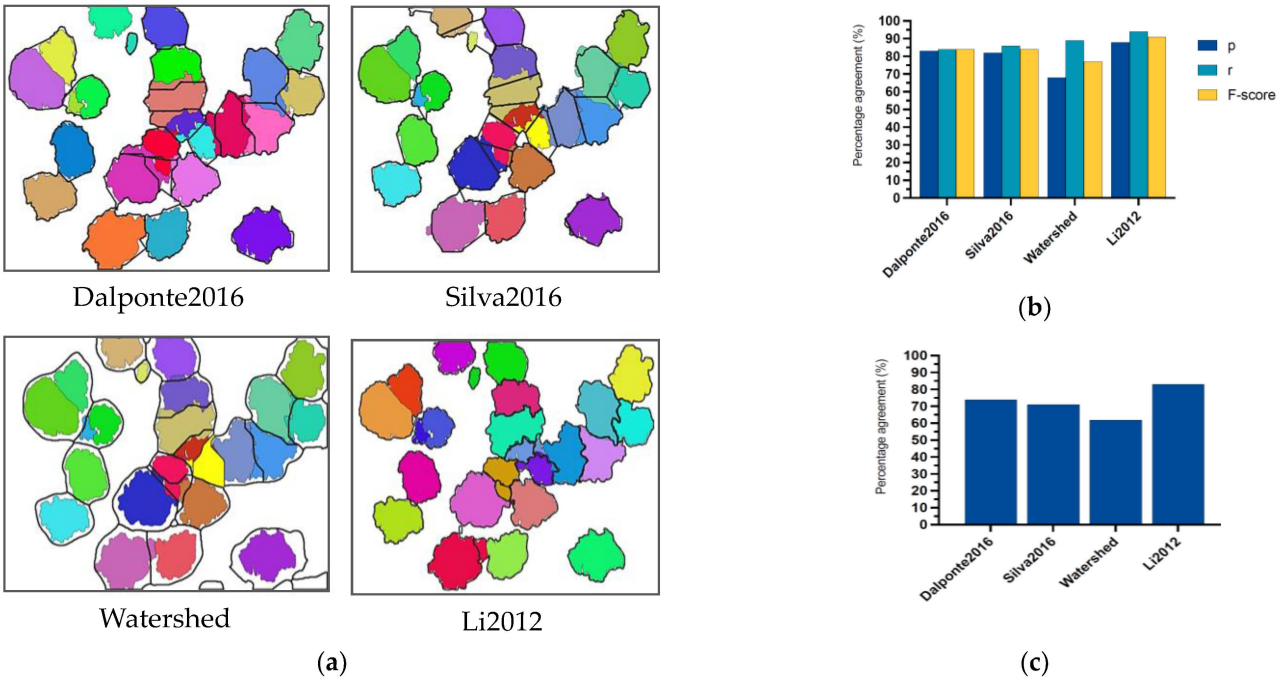

Figure 10. Segmentation results: (**a**) Reference segmentation (color fill) with respect to the segmentation algorithms (vector overlay), (**b**) precision, recall, and F1-score and (**c**) IoU.

The optimal segmentation methodology was defined, which is based on generating seeds with LMF over the CHM and performing the segmentation with the Li2012 algorithm (σ = 7 and r = 6 for Taburiente), the procedure was applied to the complete dataset of Taburiente and Garajonay providing the results displayed in Figure 11. Note that for Garajonay, it is necessary to adjust the parameters of the tree detection LMF to obtain seeds adapted to this different scenario. Field data were used with the identification of tree locations (Figure 2b). Several seed datasets were generated for segmentation by varying the value of the Gaussian smoothing factor (σ). The results obtained, as expected, were not precise with respect to location given by the ground truth due to the complexity of Garajonay, where even a manual segmentation is not possible, as tree crowns are completely mixed and their boundaries are indistinguishable, whether in multispectral images, orthophotos, or using the LiDAR data itself. The value of σ = 4 was selected since it presents the most similar seed density (110 out of the 154 trees), but the seeds location does not match the real location of trees, nor do they follow a similar spatial pattern.

Once the segmentation is completed, and given the three-dimensional nature of the data handled, it is possible to obtain different metrics related to each individual tree, such as height, crown area, and volume. In addition, if desired, it is also possible to derive metrics at the forest mass level, such as canopy cover, gap fraction, etc. For example, in the Taburiente scene, the average values of height, area, and volume of each tree were

15.5 m, 46.8 m^2, and 274.2 m^3, respectively. Figure 12 shows the metrics related to the forest structure of Taburiente extracted at the individual tree level.

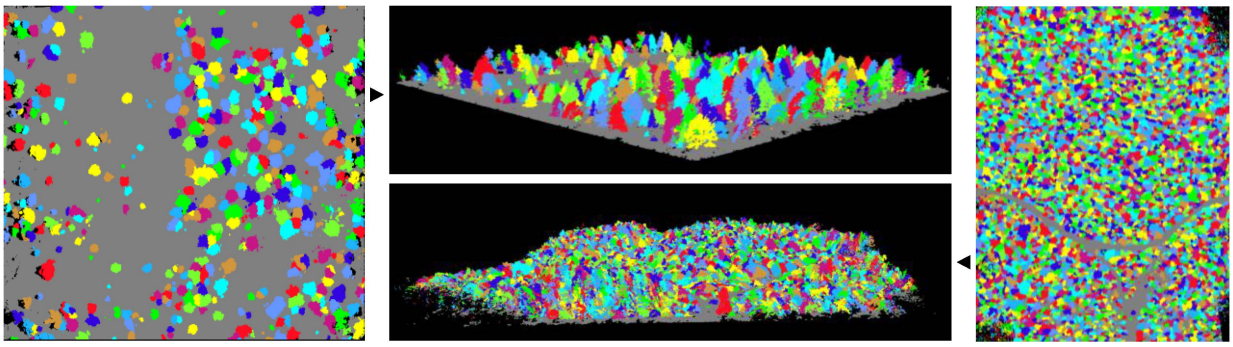

Figure 11. Individual tree segmentation for Caldera de Taburiente (**left**/**top**) and Garajonay (**right**/**bottom**) parks.

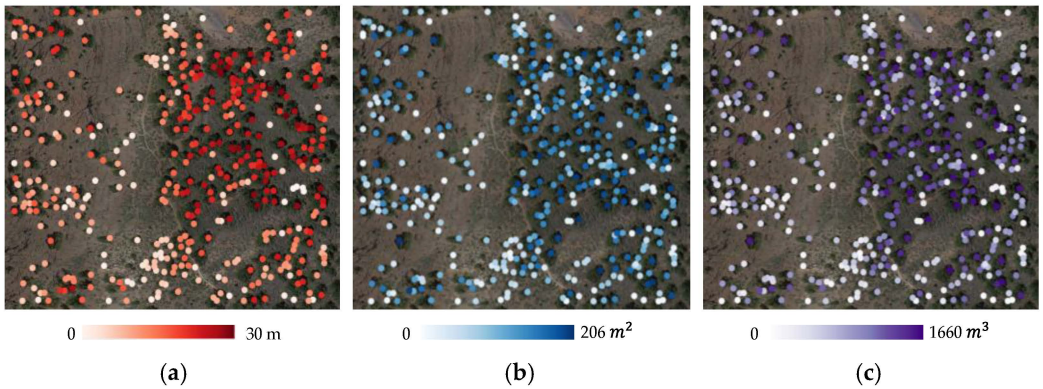

Figure 12. Forest metrics of Taburiente: (**a**) height, (**b**) area, and (**c**) volume.

4. Discussion

Protected area managers leverage LiDAR data as a powerful tool for informed decision-making and effective conservation planning, facilitating accurate assessments of forest health, biodiversity, and carbon storage capabilities. By providing highly detailed and accurate three-dimensional representations of terrain, vegetation structure, and forest composition, LiDAR enables managers to assess ecological conditions with unprecedented precision. This technology is particularly valuable for mapping biodiversity hotspots, identifying habitat corridors, and detecting changes in vegetation over time. Additionally, LiDAR's ability to penetrate canopies allows for the monitoring of understory dynamics, which are critical for evaluating habitat suitability for various species. In natural areas with difficult-to-access terrains, LiDAR also offers a non-invasive means to collect data, reducing the need for extensive fieldwork and minimizing human impact on sensitive ecosystems. Moreover, LiDAR supports the assessment of erosion risks and the mapping of potential restoration sites, ensuring the long-term resilience of ecosystems.

Specifically, ALS is particularly useful for regional planning, allowing managers to identify areas at risk of degradation or requiring restoration, while ULS, on the other hand, excels in mapping fine-scale attributes. In particular, segmenting individual trees enables detailed assessments of tree structure, health, and spatial distribution, which are essential for sustainable forestry practices and ecological research. In our study, high-quality and high-density LiDAR data were used, and a significant effort was made to generate accurate canopy height models and normalized point clouds, as these input datasets influence the accuracy of the segmentation algorithms. Two quite different ecosystems were examined: (i) Taburiente, an area populated by conifers with a moderate degree of overlapping in the tree crowns and some areas with gaps between trees, and (ii) Garajonay, a very complex

area dominated by laurel and fayal-brezal forests with an extremely high density of trees and very complex morphologies, as shown in Figure 2b. Consequently, good results in Garajonay could not be achieved, even having the precise location of the trees and using advanced processing techniques. Figure 13 shows examples of the true color composite and vertical profiles to emphasize the complexity of the area to identify individual trees.

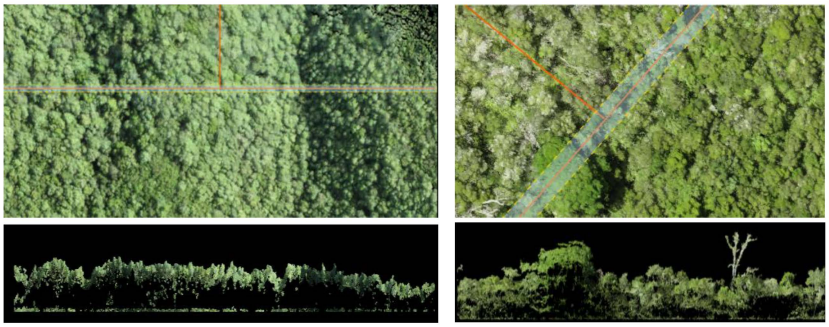

Figure 13. Vertical profiles at the Garajonay National Park.

Despite its advanced capabilities, LIDAR-based tree segmentation faces several limitations. The complexity of forest canopies, especially in dense and multilayered environments, poses significant challenges for accurately distinguishing individual trees due to overlapping crowns and varying tree heights. Computational demands are another concern, as point-based methods that leverage detailed 3D information require substantial processing power and sophisticated algorithms. The quality and resolution of LiDAR data also play a crucial role; lower-resolution data can lead to under-segmentation, where multiple trees are incorrectly grouped together. Additionally, the sensitivity of segmentation algorithms to different parameter settings can result in inconsistent outcomes across various forest types. Finally, detecting subcanopy trees remains less accurate compared to dominant canopy trees, introducing potential biases in forest structure analysis. These limitations highlight the need for ongoing advancements in LiDAR technology and algorithm development to enhance the precision and reliability of tree segmentation in complex forest ecosystems.

Regarding the LiDAR processing models, they were selected after a preliminary review of the state of the art (Table 1). We selected two software tools (LIDAR360 and LidR) that encompass most of the preprocessing and segmentation algorithms used nowadays. Certainly, apart from the ones included, other software tools are available, like FUSION, LASTools, SAGA, etc., but after being tested on a small portion of a dataset, they were disregarded in the detailed comparison of segmentation algorithms as they were not appropriate or provided redundant information. For example, FUSION [52], developed by the USDA Forest Service, is widely used to help researchers understand, explore, and analyze LiDAR data. It includes a comprehensive set of command-line tools that help users assess the overall quality and completeness of LiDAR data. However, this software is primarily used for forest-stand level analysis with ALS data, and it is not optimized for accurate analysis with high-density LiDAR data. In this context, it includes the function *CanopyMaxima* for individual tree segmentation that scans the CHM and identifies the highest point within a variable window. In this case, the window size is determined using a 5-degree polynomial equation [53]. The algorithm works best for conifer trees that are relatively isolated, but in dense stands, trees cannot be properly separated. Also, performance is not accurate in deciduous forests because the crown shape tends to be rounded, and crowns tend to overlap. In any case, we tested FUSION on a very small portion of the Taburiente dataset, and results were quite acceptable, but as the other two software tools provided the same algorithm with better performance and computational speed, we did not include it in the comparison. Basically, the same observations apply to the other software tested.

According to the results presented in Figure 10, it was clear that point cloud-based clustering algorithms exhibit higher accuracy compared with the CHM segmentation tech-

niques. For CHM-based segmentation, our study found that the Dalponte2016 model outperformed others in line with other works [20,21,54,55], which contrasts with the findings of other authors [19,26,30] where the watershed approach was deemed the most effective. This discrepancy highlights that the optimal crown delineation model may vary depending on factors such as point density, forest conditions, and tree species. On the other hand, the Li2012 point cloud region-growing algorithm demonstrated high tree detection rates, successfully identifying most trees, consistent with the results reported, for example, by Saeed et al. (2024) [21], Wang et al. (2024) [23], Ma et al. (2022) [32], or Pirotti et al. (2017) [55]. As indicated, deep learning methods are ready to play an increasingly significant role in the segmentation of individual trees using LiDAR data. By leveraging convolutional neural networks, graph neural networks, or transformers, deep learning models can be trained to automatically segment individual trees with minimal manual intervention, even in heterogeneous forest environments. With the greater availability of LiDAR data and reference-annotated datasets, the ability of deep learning algorithms to scale, generalize across different forest types, and improve with additional training data will likely revolutionize forest inventory and ecosystem management [56].

The development of reference datasets with individual trees segmented using LiDAR data is essential for advancing the field of forest remote sensing [57]. Apart from supporting the development of new deep learning algorithms by providing a reliable source of training and validation data, these datasets provide a standardized benchmark that allows researchers to systematically evaluate and compare the performance of different segmentation algorithms. Without such reference datasets, it is challenging to assess the true accuracy and reliability of various methods, as inconsistencies in data quality, forest types, and preprocessing techniques can lead to significant variations in results.

Finally, another aspect to consider when comparing results in different works is the use of accuracy metrics for individual tree segmentation. This lack of standardization can lead to difficulties in comparing results across different studies, making it challenging to assess the true performance of segmentation algorithms. For example, most of the studies included in Table 1 only include metrics that highlight tree detection rather than also evaluating its crown area or other parameters. Our work addresses both aspects, with specific metrics in all cases. On the other hand, inconsistencies between studies exist not only in the selection of accuracy metrics but also in their definitions [8,58]. For example, Intersection over Union (IoU) is set at multiple levels in some studies, contrasting with the common choice of 50%. A higher IoU threshold requires a true positive prediction to overlap more accurately with the ground truth area. Thus, introducing multiple IoU thresholds results in different ways of calculating metrics.

5. Conclusions

Forests provide numerous social, economic, and environmental benefits, and, consequently, solutions are needed to monitor them precisely. In this regard, LiDAR offers high-resolution, three-dimensional data that enables precise mapping of forest structure, including canopy height, density, and biomass. This detailed information facilitates more accurate assessments of forest health, biodiversity, and carbon storage capabilities. By leveraging LiDAR data, forest managers can implement targeted conservation strategies and monitor changes over time with greater accuracy.

In this study, we developed and evaluated a comprehensive methodology for accurately segmenting individual trees using UAV-LiDAR data. High-density point clouds were recorded from two different forest zones (Garajonay and Caldera de Taburiente national parks) to assess the overall methodology. Regarding the preprocessing step, three algorithms for ground point classification were tested, as well as three interpolation methods to generate the Digital Elevation Model. Following a comprehensive review of recent publications, four tree segmentation algorithms were selected and evaluated under various parameter settings. Visual and quantitative accuracy metrics were employed to assess the performance of these algorithms for tree detection and crown delineation. By comparing the

segmentation results against a reference dataset, created through manual segmentation and field data, we identified the optimal parameters and techniques. The experimental results revealed that the Li2012 point cloud clustering algorithm achieved the best performance, with Dalponte2016 CHM-based segmentation ranking second.

The findings of this work demonstrate that it is feasible to detect and delineate individual trees with a high degree of accuracy, depending on the complexity of the forest environment. However, the results underscore the critical importance of implementing appropriate preprocessing techniques and selecting the most suitable segmentation algorithms. Additionally, fine-tuning of algorithm parameters plays a key role in optimizing segmentation performance, ensuring that each tree is accurately identified and its crown properly delineated.

In any case, it is important to emphasize that a critical challenge of LiDAR systems is accurately segmenting forest structures in areas with dense vegetation or multi-layered canopies. Traditional algorithms often struggle with these complexities, leading to inaccuracies in detecting understory vegetation or distinguishing between overlapping tree crowns. To overcome these challenges, recent works focus on integrating LiDAR with advanced deep learning techniques, as they can adapt to the complexity of forest structures. However, to ensure their applicability across different forest types, building diverse datasets for training deep learning models is another critical step. Additionally, incorporating multisensory data, such as hyperspectral or multispectral imagery, into deep learning frameworks could further enhance the ability to extract both structural and spectral information of forest ecosystems. In this context, our ongoing project focuses on developing new annotated datasets, spanning diverse habitats, to incorporate deep learning techniques for processing multimodal data obtained from LiDAR (Zenmuse-L1/2) and multispectral (MicaSense RedEdge Dual) sensors. These efforts are aimed at producing systematic and validated above-ground biomass products.

Author Contributions: Conceptualization, J.M. and M.S.; methodology, J.M.; software, M.S.; validation, J.M., L.A., F.M. and D.R.-E.; formal analysis, M.S.; investigation, J.M. and M.S.; writing—original draft preparation, J.M.; writing—review and editing, M.S., L.A., F.M., D.R.-E. and F.E.; visualization, J.M. and M.S.; supervision, F.M., D.R.-E., F.E. and L.A.; project administration, D.R.-E. All authors have read and agreed to the published version of the manuscript.

Funding: This work has been funded by the Spanish Organismo Autónomo Parques Nacionales (Project SPIP2022-02897).

Data Availability Statement: The ULS dataset from Taburiente, presented in this study to benchmark tree segmentation algorithms, is openly available at https://doi.org/10.5281/zenodo.14051045 (accessed on 29 October 2024).

Acknowledgments: We would like to thank the director of the Garajonay National Park, Ángel Fernández, for his excellent support during the development of this work. We also would like to thank the Instituto Geográfico Nacional (IGN), in the context of the PNOA-LIDAR project, for the provision of the DEM corresponding to the 2nd LIDAR Coverage (Product: PNOA-2015-CANAR-LG-280-3112-ORT-CLA) in Garajonay.

Conflicts of Interest: The authors declare no conflicts of interest.

References

1. Eugenio, F.C.; Da Silva, S.D.P.; Fantinel, R.A.; De Souza, P.D.; Felippe, B.M.; Romua, C.L.; Elsenbach, E. Remotely Piloted Aircraft Systems to Identify Pests and Diseases in Forest Species: The global state of the art and future challenges. *IEEE Geosci. Remote Sens. Mag.* **2022**, *10*, 320–333. [CrossRef]
2. Duan, P.; Wang, Y.; Yin, P. Remote Sensing Applications in Monitoring of Protected Areas: A Bibliometric Analysis. *Remote Sens.* **2020**, *12*, 772. [CrossRef]
3. Kattenborn, T.; Leitloff, J.; Schiefer, F.; Hinz, S. Review on Convolutional Neural Networks (CNN) in vegetation remote sensing. *ISPRS J. Photogramm. Remote Sens.* **2021**, *173*, 24–49. [CrossRef]

4. Vandendaele, B.; Fournier, R.A.; Vepakomma, U.; Pelletier, G.; Lejeune, P.; Martin-Ducup, O. Estimation of Northern Hardwood Forest Inventory Attributes Using UAV Laser Scanning (ULS): Transferability of Laser Scanning Methods and Comparison of Automated Approaches at the Tree- and Stand-Level. *Remote Sens.* **2021**, *13*, 2796. [CrossRef]
5. Tan, S.; Zhang, Y.; Qi, J.; Su, Y.; Ma, Q.; Qiu, J. Exploring the Potential of GEDI in Characterizing Tree Height Composition Based on Advanced Radiative Transfer Model Simulations. *J. Remote Sens.* **2024**, *4*, 0132. [CrossRef]
6. Rai, N.; Ma, Q.; Poudel, K.P.; Himes, A.; Meng, Q. Evaluating the Uncertainties in Forest Canopy Height Measurements Using ICESat-2 Data. *J. Remote Sens.* **2024**, *4*, 0160. [CrossRef]
7. Ke, Y.; Quackenbush, L.J. A review of methods for automatic individual tree-crown detection and delineation from passive remote sensing. *Int. J. Remote Sens.* **2011**, *32*, 4725–4747. [CrossRef]
8. Zhen, Z.; Quackenbush, L.J.; Zhang, L. Trends in Automatic Individual Tree Crown Detection and Delineation—Evolution of LiDAR Data. *Remote Sens.* **2016**, *8*, 333. [CrossRef]
9. Rocha, K.D.; Silva, C.A.; Cosenza, D.N.; Mohan, M.; Klauberg, C.; Schlickmann, M.B.; Xia, J.; Leite, R.V.; Almeida, D.R.A.d.; Atkins, J.W.; et al. Crown-Level Structure and Fuel Load Characterization from Airborne and Terrestrial Laser Scanning in a Longleaf Pine (*Pinus palustris* Mill.) Forest Ecosystem. *Remote Sens.* **2023**, *15*, 1002. [CrossRef]
10. Li, S.; Brandt, M.; Fensholt, R.; Kariryaa, A.; Igel, C.; Gieseke, F.; Nord-Larsen, T.; Oehmcke, S.; Carlsen, A.H.; Junttila, S.; et al. Deep learning enables image-based tree counting, crown segmentation, and height prediction at national scale. *PNAS Nexus* **2023**, *2*, pgad076. [CrossRef]
11. Freudenberg, M.; Magdon, P.; Nölke, N. Individual tree crown delineation in high-resolution remote sensing images based on U-Net. *Neural Comput. Appl.* **2022**, *34*, 22197–22207. [CrossRef]
12. Chehreh, B.; Moutinho, A.; Viegas, C. Latest Trends on Tree Classification and Segmentation Using UAV Data—A Review of Agroforestry Applications. *Remote Sens.* **2023**, *15*, 2263. [CrossRef]
13. Zhao, H.; Morgenroth, J.; Pearse, G.; Schindler, J. A Systematic Review of Individual Tree Crown Detection and Delineation with Convolutional Neural Networks (CNN). *Curr. For. Rep.* **2023**, *9*, 149–170. [CrossRef]
14. Dersch, S.; Schöttl, A.; Krzystek, P.; Heurich, M. Semi-supervised multi-class tree crown delineation using aerial multispectral imagery and lidar data. *ISPRS J. Photogramm. Remote Sens.* **2024**, *216*, 154–167. [CrossRef]
15. Lin, Y.; Li, H.; Jing, L.; Ding, H.; Tian, S. Individual Tree Crown Delineation Using Airborne LiDAR Data and Aerial Imagery in the Taiga–Tundra Ecotone. *Remote Sens.* **2024**, *16*, 3920. [CrossRef]
16. Luo, T.; Rao, S.; Ma, W.; Song, Q.; Cao, Z.; Zhang, H.; Xie, J.; Wen, X.; Gao, W.; Chen, Q.; et al. YOLOTree—Individual Tree Spatial Positioning and Crown Volume Calculation Using UAV-RGB Imagery and LiDAR Data. *Forests* **2024**, *15*, 1375. [CrossRef]
17. Jarahizadeh, S.; Salehi, B. Deep Learning Analysis of UAV Lidar Point Cloud for Individual Tree Detecting. In Proceedings of the 2024 IEEE International Geoscience and Remote Sensing Symposium, Athens, Greece, 7–12 July 2024. [CrossRef]
18. Xiang, B.; Wielgosz, M.; Kontogianni, T.; Peters, T.; Puliti, S.; Astrup, R.; Schindler, K. Automated Forest inventory: Analysis of high-density airborne LiDAR point clouds with 3D deep learning. *Remote Sens. Environ.* **2024**, *305*, 114078. [CrossRef]
19. Yan, Y.; Lei, J.; Jin, J.; Shi, S.; Huang, Y. Unmanned Aerial Vehicle–Light Detection and Ranging-Based Individual Tree Segmentation in *Eucalyptus* spp. Forests: Performance and Sensitivity. *Forests* **2024**, *15*, 209. [CrossRef]
20. Zhang, C.; Song, C.; Zaforemska, A.; Zhang, J.; Gaulton, R.; Dai, W.; Xiao, W. Individual tree segmentation from UAS Lidar data based on hierarchical filtering and clustering. *Int. J. Digit. Earth* **2024**, *17*, 2356124. [CrossRef]
21. Saeed, T.; Hussain, E.; Ullah, S.; Iqbal, J.; Atif, S.; Yousaf, M. Performance evaluation of individual tree detection and segmentation algorithms using ALS data in Chir Pine (*Pinus roxburghii*) forest. *Remote Sens. Appl. Soc. Environ.* **2024**, *34*, 101178. [CrossRef]
22. Yu, J.; Lei, L.; Li, Z. Individual Tree Segmentation Based on Seed Points Detected by an Adaptive Crown Shaped Algorithm Using UAV-LiDAR Data. *Remote Sens.* **2024**, *16*, 825. [CrossRef]
23. Wang, L.; Zhang, R.; Zhang, L.; Yi, T.; Zhang, D.; Zhu, A. Research on Individual Tree Canopy Segmentation of *Camellia oleifera* Based on a UAV-LiDAR System. *Agriculture* **2024**, *14*, 364. [CrossRef]
24. Wielgosz, M.; Puliti, S.; Xiang, B.; Schindler, K.; Astrup, R. SegmentAnyTree: A sensor and platform agnostic deep learning model for tree segmentation using laser scanning data. *arXiv* **2024**, arXiv:2401.15739. [CrossRef]
25. Liu, Y.; Chen, D.; Fu, S.; Mathiopoulos, P.T.; Sui, M.; Na, J.; Peethambaran, J. Segmentation of Individual Tree Points by Combining Marker-Controlled Watershed Segmentation and Spectral Clustering Optimization. *Remote Sens.* **2024**, *16*, 610. [CrossRef]
26. Nemmaoui, A.; Aguilar, F.J.; Aguilar, M.A. Benchmarking of Individual Tree Segmentation Methods in Mediterranean Forest Based on Point Clouds from Unmanned Aerial Vehicle Imagery and Low-Density Airborne Laser Scanning. *Remote Sens.* **2024**, *16*, 3974. [CrossRef]
27. Xiang, B.; Peters, T.; Kontogianni, T.; Vetterli, F.; Puliti, S.; Astrup, R.; Schindler, K. Towards Accurate Instance Segmentation in Large-Scale LiDAR Point Clouds. *ISPRS Ann. Photogramm. Remote Sens. Spatial Inf. Sci.* **2023**, *X-1/W1-2023*, 605–612. [CrossRef]
28. Chen, X.; Wang, R.; Shi, W.; Li, X.; Zhu, X.; Wang, X. An Individual Tree Segmentation Method That Combines LiDAR Data and Spectral Imagery. *Forests* **2023**, *14*, 1009. [CrossRef]
29. You, H.; Tang, X.; You, Q.; Liu, Y.; Chen, J.; Wang, F. Study on the Differences between the Extraction Results of the Structural Parameters of Individual Trees for Different Tree Species Based on UAV LiDAR and High-Resolution RGB Images. *Drones* **2023**, *7*, 317. [CrossRef]
30. Tao, Z.; Yi, L.; Wang, Z.; Zheng, X.; Xiong, S.; Bao, A.; Xu, W. Remote Sensing Parameter Extraction of Artificial Young Forests under the Interference of Undergrowth. *Remote Sens.* **2023**, *15*, 4290. [CrossRef]
31. Liu, Y.; You, H.; Tang, X.; You, Q.; Huang, Y.; Chen, J. Study on Individual Tree Segmentation of Different Tree Species Using Different Segmentation Algorithms Based on 3D UAV Data. *Forests* **2023**, *14*, 1327. [CrossRef]

32. Ma, K.; Chen, Z.; Fu, L.; Tian, W.; Jiang, F.; Yi, J.; Du, Z.; Sun, H. Performance and Sensitivity of Individual Tree Segmentation Methods for UAV-LiDAR in Multiple Forest Types. *Remote Sens.* **2022**, *14*, 298. [CrossRef]
33. Farajelahi, B.; Eya, F.F.; Arefi, H. Forest modeling and inventory estimation using lidar data. *ISPRS Ann. Photogramm. Remote Sens. Spatial Inf. Sci.* **2023**, *X-4/W1-2022*, 159–164. [CrossRef]
34. Corte, A.P.D.; da Cunha Neto, E.M.; Rex, F.E.; Souza, D.; Behling, A.; Mohan, M.; Sanquetta, M.N.I.; Silva, C.A.; Klauberg, C.; Sanquetta, C.R.; et al. High-Density UAV-LiDAR in an Integrated Crop-Livestock-Forest System: Sampling Forest Inventory or Forest Inventory Based on Individual Tree Detection (ITD). *Drones* **2022**, *6*, 48. [CrossRef]
35. Múgica, M.; Puertas, J.; Martínez, C.; García, D.; Gómez-Limón, J. *EUROPARC-España. Anuario 2023 del Estado de las Áreas Protegidas en España*; Fundación Fernando González Bernáldez: Madrid, Spain, 2024.
36. Gobierno de Canarias. Planes y Normas de los Espacios Naturales Protegidos. Available online: https://www.gobiernodecanarias.org/planificacionterritorial/materias/informacion-territorial/enp/ (accessed on 4 September 2024).
37. Marcello, J.; Eugenio, F.; Rodríguez-Esparragón, D.; Marqués, F. Assessment of Forest Degradation Using Multitemporal and Multisensor Very High Resolution Satellite Imagery. In Proceedings of the 2023 IEEE International Geoscience and Remote Sensing Symposium, Pasadena, CA, USA, 16–21 July 2023. [CrossRef]
38. Zhang, K.; Chen, S.C.; Whitman, D.; Shyu, M.L.; Yan, J.; Zhang, C. A progressive morphological filter for removing nonground measurements from airborne LIDAR data. *IEEE Trans. Geosci. Remote Sensing* **2003**, *41*, 872–882. [CrossRef]
39. Zhang, W.; Qi, J.; Wan, P.; Wang, H.; Xie, D.; Wang, X.; Yan, G. An Easy-to-Use Airborne LiDAR Data Filtering Method Based on Cloth Simulation. *Remote Sens.* **2016**, *8*, 501. [CrossRef]
40. Chen, N.; Wang, N.; He, Y.; Ding, X.; Kong, J. An improved progressive triangular irregular network densification filtering algorithm for airborne LiDAR data. *Front Earth Sci.* **2023**, *10*, 1015153. [CrossRef]
41. Geographic Information Science & Technology Body of Knowledge. Available online: https://gistbok-ltb.ucgis.org/page/24/concept/7310 (accessed on 29 October 2024).
42. Lu, G.Y.; Wong, D.W. An adaptive inverse-distance weighting spatial interpolation technique. *Comput. Geosci.* **2008**, *34*, 1044–1055. [CrossRef]
43. Lloyd, C.D.; Atkinson, P.M. Deriving DSMs from LiDAR data with kriging. *Int. J. Remote Sens.* **2002**, *23*, 2519–2524. [CrossRef]
44. Popescu, S.C.; Wynne, R.H. Seeing the trees in the forest: Using lidar and multispectral data fusion with local filtering and variable window size for estimating tree height. *Photogramm. Eng. Remote Sens.* **2004**, *70*, 589–604. [CrossRef]
45. Ortiz Zamora, F.G. Procesamiento Morfológico de Imágenes en Color. Aplicación a la Reconstrucción Geodésica. Ph.D. Thesis, Universidad de Alicante, Alicante, Spain, 2002.
46. Dalponte, M.; Coomes, D.A. Tree-centric mapping of forest carbon density from airborne laser scanning and hyperspectral data. *Methods Ecol. Evol.* **2016**, *7*, 1236–1245. [CrossRef]
47. Silva, C.A.; Hudak, A.T.; Vierling, L.A.; Loudermilk, E.L.; O'Brien, J.J.; Jack, S.B.; Gonzalez-Beneque, C.; Hiers, J.K.; Lee, H.; Falkowski, M.J.; et al. Imputation of Individual Longleaf Pine (*Pinus palustris* Mill.) Tree Attributes from Field and LiDAR Data. *Can. J. Remote Sens.* **2016**, *42*, 554–573. [CrossRef]
48. Chen, Q.; Baldocchi, D.; Gong, P.; Kelly, M. Isolating Individual Trees in a Savanna Woodland Using Small Footprint Lidar Data. *Photogramm. Eng. Remote Sens.* **2006**, *72*, 923–932. [CrossRef]
49. Li, W.; Guo, Q.; Jakubowski, M.K.; Kelly, M. A new method for segmenting individual trees from the lidar point cloud. *Photogramm. Eng. Remote Sens.* **2012**, *78*, 75–84. [CrossRef]
50. Yang, J.; Gan, R.; Luo, B.; Wang, A.; Shi, S.; Du, L. An Improved Method for Individual Tree Segmentation in Complex Urban Scenes Based on Using Multispectral LiDAR by Deep Learning. *IEEE J. Sel. Top. Appl. Earth Obs. Remote Sens.* **2024**, *17*, 6561–6576. [CrossRef]
51. Centro de Descargas. Organismo Autónomo Centro Nacional de Información Geográfica. Available online: https://centrodedescargas.cnig.es/CentroDescargas/index.jsp (accessed on 3 March 2024).
52. FUSION. Forest Service. Department of Agriculture. Available online: http://forsys.cfr.washington.edu/fusion/fusionlatest.html (accessed on 13 April 2023).
53. Kini, A.U.; Popescu, S.C. TreeVaW: A Versatile Tool for Analyzing Forest Canopy LiDAR Data—A Preview with an Eye towards Future. In Proceedings of the ASPRS 2004 Fall Conference, Kansas City, MO, USA, 12–16 September 2004.
54. Cao, Y.; Ball, J.G.C.; Coomes, D.A.; Steinmeier, L.; Knapp, N.; Wilkes, P.; Disney, M.; Calders, K.; Burt, A.; Lin, Y.; et al. Benchmarking airborne laser scanning tree segmentation algorithms in broadleaf forests shows high accuracy only for canopy trees. *Int. J. Appl. Earth Obs. Geoinf.* **2023**, *123*, 103490. [CrossRef]
55. Pirotti, F.; Kobal, M.; Roussel, J.R. A Comparison of Tree Segmentation Methods Using Very High Density Airborne Laser Scanner Data. *Int. Arch. Photogramm. Remote Sens. Spatial Inf. Sci.* **2017**, *XLII-2/W7*, 285–290. [CrossRef]
56. Henrich, J.; van Delden, J. Towards general deep-learning-based tree instance segmentation models. *arXiv* **2024**, arXiv:2405.02061v1. [CrossRef]
57. Fu, Y.; Niu, Y.; Wang, L.; Li, W. Individual-Tree Segmentation from UAV–LiDAR Data Using a Region-Growing Segmentation and Supervoxel-Weighted Fuzzy Clustering Approach. *Remote Sens.* **2024**, *16*, 608. [CrossRef]
58. Kim, D.-H.; Ko, C.-U.; Kim, D.-G.; Kang, J.-T.; Park, J.-M.; Cho, H.-J. Automated Segmentation of Individual Tree Structures Using Deep Learning over LiDAR Point Cloud Data. *Forests* **2023**, *14*, 1159. [CrossRef]